

SCIENTIFIC REPORTS



OPEN

High frequency of +1 programmed ribosomal frameshifting in *Euplotes octocarinatus*

Ruanlin Wang¹, Jie Xiong², Wei Wang¹, Wei Miao² & Aihua Liang¹

Received: 08 October 2015
 Accepted: 18 January 2016
 Published: 19 February 2016

Programmed -1 ribosomal frameshifting (-1 PRF) has been identified as a mechanism to regulate the expression of many viral genes and some cellular genes. The slippery site of -1 PRF has been well characterized, whereas the $+1$ PRF signal and the mechanism involved in $+1$ PRF remain poorly understood. Previous study confirmed that $+1$ PRF is required for the synthesis of protein products in several genes of ciliates from the genus *Euplotes*. To accurately assess the frequency of genes requiring frameshift in *Euplotes*, the macronuclear genome and transcriptome of *Euplotes octocarinatus* were analyzed in this study. A total of 3,700 $+1$ PRF candidate genes were identified from 32,353 transcripts, and the gene products of these putative $+1$ PRFs were mainly identified as protein kinases. Furthermore, we reported a putative suppressor tRNA of UAA which may provide new insights into the mechanism of $+1$ PRF in euplotids. For the first time, our transcriptome-wide survey of $+1$ PRF in *E. octocarinatus* provided a dataset which serves as a valuable resource for the future understanding of the mechanism underlying $+1$ PRF.

As a typical ciliate, *Euplotes octocarinatus* exhibits nuclear dimorphism [micronucleus (MIC) and macronucleus (MAC)]. The MIC is diploid and transcriptionally inert during most of its life cycle, enabling the transmission of genetic information between generations by sexual reproduction. The MAC is considered the somatic nucleus, which is transcriptionally active during the vegetative growth¹. During conjugation, the MAC is degraded and a new MAC is developed from the zygote nucleus accompanied by DNA rearrangements. Similar to that of other hypotrichous ciliates, the MAC of *E. octocarinatus* contains abundant gene-sized DNA molecules ('nanochromosome', with mean length ~ 2 kb), each of which is differentially amplified². All nanochromosomes have telomeric repeats 5'-(C₄A₄)_n-3' at their ends³.

The following unique features distinguish *Euplotes* from other ciliates: 1) the conventional stop codon UGA is reassigned as cysteine⁴ or selenocysteine⁵, which means that only the UAA and UAG are used as stop codons in *Euplotes*; and 2) the high frequency of $+1$ programmed ribosomal frameshifting (PRF) in *Euplotes*⁶. PRF is a recoding event by which the translating ribosome switches from the initial (0) reading frame to the -1 or $+1$ reading frame at a specific position, and then continues its translation⁷. Although the first reported frameshifting sequence has been found in viruses, it is becoming increasingly apparent that PRF is also widespread and likely exists in all branches of life from bacteria to higher eukaryotes^{8–10}.

On the basis of the reading frame shift, two main PRFs (-1 and $+1$) were reported in viruses and other cellular organisms. The -1 PRF is prevalent and abundant and the most well-defined -1 PRF phenomena are directed by an mRNA sequence motif composed of the following three crucial elements¹¹: 1) the so-called slippery sequence composed of seven nucleotides; 2) a short spacer sequence (usually less than 12 nt); and 3) a downstream stimulatory structure (usually a pseudoknot or a stem-loop). Compared with -1 PRF, $+1$ PRF has fewer examples found in bacteria, fungi, mammals and ciliated protozoa of *Euplotes*. In the majority of bacteria, $+1$ PRF reportedly regulates the expression of release factor 2 (RF2)^{12,13}; in fungi and mammals, $+1$ PRF purportedly regulates the expression of ornithine decarboxylase antizyme (OAZ), the negative regulator of cellular polyamine levels^{14,15}.

Unlike -1 PRF, which has only one well-understood type of frameshift signal, $+1$ PRF involves highly diverse mechanisms. In *Escherichia coli*, RF2 autoregulates its production by the in-frame UGA premature

¹Key Laboratory of Chemical Biology and Molecular Engineering of Ministry of Education, Institute of Biotechnology, Shanxi University, Taiyuan 030006, China. ²Key Laboratory of Aquatic Biodiversity and Conservation, Institute of Hydrobiology, Chinese Academy of Sciences, Wuhan 430072, China. Correspondence and requests for materials should be addressed to A.L. (email: aliang@sxu.edu.cn)

termination codon found within the slippery site U CUU UGA. Peptide chain termination is efficient when adequate RF2 is present, thereby suppressing +1 PRF and limiting its translational production. However, low RF2 levels result in the inefficient recognition of the UGA codon and thus increased efficiency of +1 PRF, thereby allowing the expression of the RF2 protein¹⁶. In addition, a Shine–Dalgarno–like (SD–like) element located upstream of the slippery site can stimulate a +1 frameshift by interacting with the anti–SD sequence on the 16S rRNA¹⁷. In eukaryotes, +1 PRF is driven by other mechanisms. In the case of human OAZ mRNA, the crucial stimulatory element is the mRNA secondary structure located downstream of the slippery sequence. Similar to RF2 from *E. coli*, the OAZ +1 frameshift is stimulated by a 0–frame UGA codon, and is also autoregulated. Ornithine decarboxylase (ODC) catalyses the first step in polyamine biosynthesis, whereas OAZ downregulates polyamine synthesis by stimulating the ubiquitin-independent degradation of ODC by the proteasome. Thus, the increased levels of polyamines cause a negative feedback on polyamine synthesis by stimulating +1 PRF, and hence OAZ synthesis¹⁸.

Euplotes contains several +1 PRF genes, such as the Tec2 transposon ORF2 protein^{19,20}, membrane occupation and recognition nexus (MORN) repeat protein, C₂H₂-type zinc finger protein, Ser/Thr protein kinase⁶, cAMP-dependent protein kinase²¹, nuclear protein kinase²², La motif protein²³, mitogen-activated protein kinase (MAPK1)^{24,25}, and the reverse transcriptase subunits of telomerase^{26–28}. All of these genes have some common features. Their slippery sequences usually have the motif 5′-AAA-TAR-3′ (where R=A or G, the underlined sequence denotes the 0–frame codons), and all genes require a +1 PRF to produce complete protein products. In addition, a previous survey⁶ of *Euplotes crassus* macronuclear genes by random sequencing has found three new putative +1 PRF genes from 23 macronuclear genes, suggesting that the frequency of genes requiring frameshifts may exceed 10%.

The present study conducted a genome-wide investigation of +1 PRF in *E. octocarinatus* through genome and transcriptome sequencing. A total of 3,700 (approximately 11%) putative +1 PRF genes were identified in *E. octocarinatus*. To the best of our knowledge, this frequency of +1 PRF is the highest found in all living organisms. Based on the functional annotation of Pfam, GO and KEGG, we systematically investigated the putative functions of +1 PRF gene products, which were mainly enriched in protein kinases. We also found a novel suppressor tRNA of UAA which is a potential key factor of +1 PRF in euplotids. This work provides the first comprehensive genome-wide investigation of +1 PRF in *E. octocarinatus*, and thus lays a foundation for further exploring the mechanism of PRF.

Results and Discussion

Constructing the transcripts of *E. octocarinatus* by genome and transcriptome sequencing.

The PRF occurs at the post-transcriptional level; thus, transcripts should first be assembled to analyse the PRF. Reference-based transcriptome assembly is reported as the best method to construct transcripts, especially full-length transcripts, from short high-throughput sequencing reads²⁹. The MAC genome and transcriptome of *E. octocarinatus* were sequenced to construct a high quality transcripts set.

In consideration of the unique properties of the highly fragmented macronuclear genome of *Euplotes*, two short paired-end sequencing libraries with insert sizes of 180 bp (100 bp × 2 by Illumina HiSeq2000 platform) and 500 bp (300 bp × 2 by Illumina Miseq platform) were constructed and sequenced. In total, about 11 gigabases (Gb) were obtained (Table S1). Several popular short-read assemblers were tested and compared to obtain full-length nanochromosomes and the minimum number of contigs simultaneously (Table 1). Finally, we adopted the strategy in Figure S1. In general, HiSeq and Miseq data were independently assembled using the assembler with the best performance. Specifically, the Miseq data (300 bp × 2) were assembled using Mira. This assembly produced a large proportion of 2–telomere contigs (61.0%) and long contigs (N50 length 2,683 bp). However, the Miseq assembly missed many nanochromosomes which were shorter than 500 bp because of the library insert size limitation (Table 1). Therefore, the HiSeq data (100 bp × 2) was independently assembled using SPAdes. This assembly produced 24.8% of 2–telomere capped contigs with a N50 length of 1,129 bp. Then, the two assemblies were merged using CAP3, and all redundant contigs were removed on the basis of the result of LASTZ (see Methods and Fig. S1). However, some telomereless contigs (5,494) shorter than 500 bp were not removed from the final assembly. We speculate that those ‘chaff’ contigs were fragments of the MIC or the inter-genic regions of some long chromosomes with a low GC content (Fig. S2).

Based on the GC content results of all contigs (Fig. S3), we suspected that the initial assembly contained a mixture of target DNA, bacterial DNA (endosymbionts of *E. octocarinatus*) and mitochondrial DNA (some sub-peaks were located behind the major peak). Therefore, a series of filters was applied to exclude the contamination (see Methods), and 1,628 bacterial contigs and 72 mitochondrial contigs were removed from the initial assembly. Finally, a total of 41,980 contigs with an average length of 2,117 bp were used as the *E. octocarinatus* MAC genome assembly, and most (70.1%) of these contigs were capped with telomeres on both ends. The completeness of the genome was supported by the assessment results (see Methods). Subsequently, we compared two reported highly fragmented macronuclear genomes^{30,31} with the *E. octocarinatus* assembly. Similar to *Oxytricha* and *Stylonychia*, few nanochromosomes were assembled at either extremities of the length distribution in *Euplotes* (Fig. 1). Only 283 were shorter than 500 bp and 15 were longer than 15 kb.

To construct the transcript set, high-throughput RNA-seq (125 bp × 2) of *E. octocarinatus* was performed (see Methods). We obtained 39,478,354 short reads, with a total length of more than 4.9 Gb through sequencing. Low-quality reads were filtered by fastq_quality_filter with the parameters -q 20 -p 80. Then high-quality reads of RNA-seq data were mapped to the *Euplotes* macronuclear genome by Tophat³², and all mapped reads were assembled using Cufflinks³³. Finally, 32,353 transcripts were generated with a mean transcript length of 1,300 bp and a N50 of 1,578 bp.

| Assembler | ABySS | SOAP | SPAdes | Mira | SPAdes | Final Assembly |
|--|------------|------------|------------|------------|------------|----------------|
| Assembler version | 1.5.1 | 2.04 | 2.5.0 | 4.0.2 | 2.5.0 | – |
| Data | HiSeq Data | HiSeq Data | HiSeq Data | MiSeq Data | MiSeq Data | – |
| Assembly size (Mb) | 83.0 | 97.8 | 84.6 | 126.2 | 107.2 | 88.9 |
| Contigs (n) | 241,146 | 180,079 | 74,880 | 56,612 | 68,352 | 41,980 |
| N50 (bp) | 1,144 | 1,650 | 2,034 | 2,683 | 2,443 | 2,947 |
| Mean contig length (bp) | 344 | 543 | 1129 | 2228 | 1,619 | 2117 |
| Max contig length (bp) | 18,818 | 17,403 | 18,769 | 53,269 | 195,456 | 53,269 |
| Number of 2-telomere contigs (n) | 13,935 | 6676 | 18,556 | 34,536 | 27,802 | 29,413 |
| Number of 1-telomere contigs (n) | 32,125 | 23,449 | 17,959 | 12,751 | 7,548 | 4,367 |
| Number of 0-telomere contigs (n) | 195,085 | 149,942 | 38,364 | 8,749 | 32,594 | 7,554 |
| Number of multi-telomere contigs | 1 | 12 | 1 | 576 | 408 | 645 |
| Number of shorter nanochromosomes (length \leq 500 bp) | 269 | 137 | 287 | 5 | 68 | 287 |
| 2-telomere contig percentage (%) | 5.8 | 3.7 | 24.8 | 61.0 | 40.7 | 70.1 |
| Total PE read coverage (%) | 82.1 | 95.9 | 98.3 | 84.7 | 90.2 | 95.9 |
| Telomeric PE read coverage (%) | 72.6 | 52.1 | 99.6 | 88.5 | 89.7 | 91.9 |

Table 1. Comparison of *Euplotes octocarinatus* macronuclear genome assemblies.

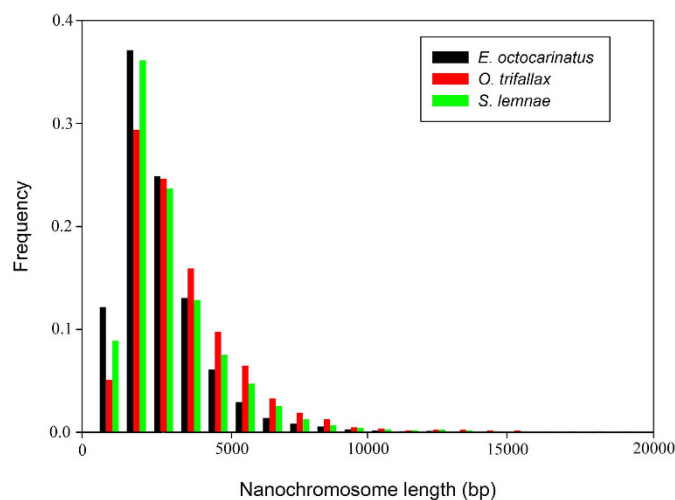


Figure 1. Length distribution of nanochromosomes of three highly fragmented macronuclear genomes. X axis is the contig length (nucleotides), Y axis is the frequency of contigs with the indicated lengths. The histograms show normalized frequencies for 29,413 nanochromosomes of *Euplotes octocarinatus*, 15,085 nanochromosomes of *Oxytricha trifallax* and 16,029 nanochromosomes of *Stylonychia lemnae*.

High frequency of +1 PRF in *E. octocarinatus*. A similarity search-based method was used to identify the +1 PRF transcripts in *E. octocarinatus*. The strategy was to find out-of-frame ORFs first and then identify the frameshift motif in the in-frame ORF which could potentially redirect ribosomes from the upstream ORF into the downstream one, resulting in the translation of a complete protein. As depicted in Fig. 2, all transcripts were aligned to the NCBI non-redundant (nr) protein database by using BLASTX with a cut-off of 10^{-5} . A total of 6,064 transcripts having two or more high score fragments with different reading frames in the same hit protein sequence were extracted on the basis of BLASTX results. Considering that the intron retention transcripts may also direct the production of out-of-frame ORFs and lead to BLASTX results similar to PRF genes, we identified and excluded intron retention transcripts by using transcriptome information. Based on the typical arrangement of +1 frameshift genes in *Euplotes*, the initial open reading frame is expected to terminate with the sequence 5'-AAA-TAR-3'. So the stop codon (TAA or TAG) was searched in the initial open reading frame, and the 'T' of the stop codon was artificially removed. Subsequently, this new *fs*-gene was aligned to the NCBI nr protein database by BLASTX again. Once a C-terminally extended protein was produced, this gene would be marked as a +1 PRF gene. Using this strategy, we identified 3,700 putative +1 PRF genes from the 32,353 *E. octocarinatus* transcripts. In addition to the 3,489 +1 PRF genes with the classical '*Euplotes* frameshift motif' (5'-AAA-TAR-3'), we also identified 211 novel +1 PRF genes with different types of slippery sequences. Among these novel +1 PRF genes, the most abundant slippery sequence motif was the 5'-TTT-TAR-3' motif with 54

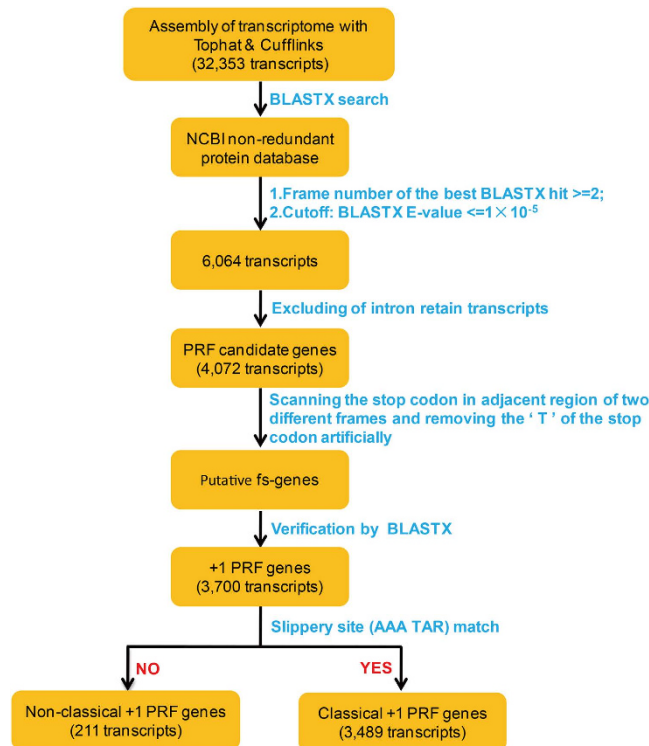


Figure 2. Pipeline of prediction of +1 programmed ribosomal frameshifted transcripts.

genes (Table S2), followed by the 5′-AAG-TAR-3′ motif with 41 genes, the 5′-AAT-TAR-3′ motif with 29 genes, and the 5′-ATT-TAR-3′ motif with 28 genes.

Thus, the present study has increased the number of previously known +1 PRF genes in *E. octocarinatus* by three orders of magnitude. As expected, two previously reported +1 PRF genes in *E. octocarinatus* – cAMP-dependent protein kinase²¹ (CUFF.28794.1) and putative nuclear protein kinases²² (CUFF.8279.1) – were identified by our pipeline, suggesting that the method we used was robust. Detailed information on the putative +1 PRF transcripts, including length, GC content, coordinates of predicted slippery site and E-value of BLASTX is presented in Table S3.

The genome-wide analysis of the *Saccharomyces cerevisiae* genome¹¹ and 1,106 complete prokaryotic genomes³⁴ suggests a high frequency of –1 PRF in these organisms. However, only a few of the +1 PRF genes have been described (Table 2). By contrast, no –1 PRF gene has been reported in *Euplotes* so far, but several +1 PRF cases have been reported. Our results showed that approximately 11.4% genes required +1 PRF to produce a functional protein in *E. octocarinatus*. Our results provide evidence supporting the notion that euplotids contain an extremely high number of genes requiring +1 frameshifts for expression at the post-transcriptional level. The observed number of +1 PRF genes was higher in *E. octocarinatus* than in other organisms (Table 2), but the true percentage of frameshifted genes in *E. octocarinatus* should be more abundant, because only 52.4% of the transcripts (16,950 of 32,353) have a homologous gene in other organisms. In specific, about half of the transcripts whose functions are unknown may also require a frameshift for expression.

Hypothetical function of +1 PRF gene products is significantly enriched in protein kinases. We systematically investigated the hypothetical function of 3,700 identified +1 PRF genes. A total of 2,336 putative +1 PRF genes were found to contain at least one protein domain by searching the Pfam database. The most abundant protein domain found in those genes was ‘Pkinase’ domain (PF00069.20), with a total of 362 genes (Table S4), followed by the ‘MORN’ domain (PF02493.15) with 265 genes, the ‘WD40’ domain (PF00400.27) with 179 genes, the ‘SHIPPO-rpt’ domain (PF07004.7) with 146 genes, and the ‘cNMP_binding’ domain (PF00027.24) with 130 genes. All putative +1 PRF genes were mapped to the Kyoto Encyclopedia of Genes and Genomes (KEGG)³⁵ pathway to investigate the biological pathways where the putative +1 PRF genes may be involved. In general, 813 genes were assigned to 282 KEGG pathways (Table S5). The pathways represented by the putative +1 PRF genes included the PI3K-Akt signalling pathway (18 members), the sphingolipid signalling pathway (14 members) and the MAPK signalling pathway (12 members). Furthermore, a total of 1,629 putative +1 PRF transcripts were annotated with at least one GO term and categorised into 26 functional groups on the basis of sequence homology (Fig. S4). In each of the three main categories, namely, GO classification cellular component, molecular function and biological process, the terms ‘cell’ and ‘cell part’, ‘binding’ and ‘catalytic’, and ‘cellular process’ were dominant, respectively.

| Organism | Evolutionary Group | Total gene number ^a | +1 PRF gene number ^b | Method & Reference |
|---|---------------------|--------------------------------|---------------------------------|---|
| <i>Homo sapiens</i> | Eukaryote (Metazoa) | 20,403 | 3 | Experimental verification ⁷⁰⁻⁷² |
| <i>Rattus norvegicus</i> | Eukaryote (Metazoa) | 23,636 | 1 | Experimental verification ⁷³ |
| <i>Mus musculus</i> | Eukaryote (Metazoa) | 22,556 | 3 | Experimental verification ^{71,72,74} |
| <i>Xenopus laevis</i> | Eukaryote (Metazoa) | 11,078 | 1 | Experimental verification ⁷⁵ |
| <i>Danio rerio</i> | Eukaryote (Metazoa) | 26,719 | 2 | Experimental verification ⁷⁶ |
| <i>Drosophila melanogaster</i> | Eukaryote (Metazoa) | 13,954 | 1 | Experimental verification ⁷⁷ |
| <i>Caenorhabditis elegans</i> | Eukaryote (Metazoa) | 20,360 | 1 | Experimental verification ⁷⁵ |
| <i>Saccharomyces cerevisiae</i> | Eukaryote (Fungi) | 5,907 | 3 | Experimental verification ^{18,78,79} |
| <i>Euplotes octocarinatus</i> | Eukaryote (Ciliate) | ~32,353 | 3,700 | Computational analysis This work |
| <i>Escherichia coli</i> | Prokaryote | 4,140 | 1 | Experimental verification ¹² |
| <i>Listeria monocytogenes</i> phage PSA | Virus | – | 2 | Experimental verification ⁸⁰ |
| <i>Influenza A virus</i> | Virus | – | 1 | Experimental verification ⁸¹ |

Table 2. Summary of +1 programmed ribosomal frameshifted genes in diverse organisms. ^aGene number retrieved from the KEGG genome statistics. ^bOnly non-transposon, protein-coding genes.

Functional annotations indicated that the putative +1 PRF genes in *E. octocarinatus* possessed various functions involved in multiple cellular processes and pathways. As reported previously, most putative +1 PRF genes encode proteins with enzymatic functions, especially protein kinases⁶. However, none of the highly expressed genes in cells have been reported to require a frameshift which is proven by the fact that the expression abundance of putative +1 PRF genes [mean fragments per kilobase of transcript per million mapped fragments (FPKM) value: 10.59] was significantly lower than that of normal genes (mean FPKM value: 44.38) ($p < 0.01$, t test). The most abundant representative proteins in the cell were ribosomal proteins. All 79 of the standard eukaryotic ribosomal proteins of *E. octocarinatus* (32 small subunit and 47 large subunit proteins) were identified and analysed, and none of them required a frameshift for expression.

A GO enrichment analysis of putative +1 PRF genes was performed to investigate the functional enrichment of putative +1 PRF genes. Results showed that the identified putative +1 PRF genes were significantly overrepresented in the regulation of various biological processes such as dephosphorylation, protein amino acid phosphorylation, and ubiquitin-dependent protein catabolic process (Fig. 3).

These results suggest that the products of these putative +1 PRF genes in *E. octocarinatus* are significantly enriched in protein kinases. Protein kinases are important regulatory components of every eukaryotic intracellular signal transduction pathway. Some protein kinases, such as MAPK1, are associated with cell proliferation and cell cycle events; MAPK1 is a homologous kinase with intestinal–cell kinases in mammals. The expression of the *MAPK1* gene requires +1 translational frameshifting in both *Euplotes raikovi*²⁴ and *Euplotes nobilii*²⁵. This *Euplotes* kinase is related to the autocrine signalling loop that promotes vegetative growth. Furthermore, the MAPK1 of *E. raikovi* resides in the nuclear apparatus, where it appears either phosphorylated in growing cells which interact in autocrine fashion with their own specific (self) signalling pheromones or dephosphorylated in cells which are induced to mate and temporarily arrest their growth by paracrine interactions with foreign (non-self) signalling pheromones²⁴. These results suggest that +1 PRF genes may have important functions in cell growth.

Suppressor tRNA may play an important role in +1 frameshifting in *E. octocarinatus*. With sufficient samples of +1 PRF genes, the conserved sequence elements which might facilitate frameshifting were checked. To search the potential conserved sequence elements, 30 bp upstream and downstream of the conserved slippery sequence motif from 4,545 predicted slippery sites were extracted and analysed using WebLogo³⁶. Consistent with a previous report, no conserved sequence element was found except the slippery site sequence 5'-WWW TAR-3' (W=A or T, Fig. 4), suggesting that frameshifting does not depend on other sequence motifs.

Klobutcher and Farabaugh³⁷ suggested that altering eRF1 to ignore UGA might impair its recognition of other termination codons in *Eupotes*. In addition, Vallabhaneni *et al.*³⁸ proved that the reassignment of UGA to Cys in *E. octocarinatus* increases +1 slippery stop frameshifting at both UAA and UAG. Based on this finding, we analysed the stop codon usage in *E. octocarinatus* at the transcriptome level, and compared the usage between the 'normal' stop codon and the slippery stop codon. Results showed that UAA was preferentially used in both the 'normal' termination signal (79.6%) and the slippery signal (89.4%) (Fig. 5A). Moreover, the frequency of UAA codon usage in slippery signal is significantly higher than that in 'normal' termination signal ($P < 0.01$, Fisher exact test) which suggested that UAA may be favourable for frameshifting in *E. octocarinatus*. The release factor recognises a tetranucleotide sequence consisting of the termination codon and its nearest 3' neighbour nucleotide in both prokaryotes and eukaryotes³⁷. Thus, we also analysed the frequency of the tetranucleotide sequence in both normal and +1 PRF slippery sites (Fig. 5B). A similar trend was found in both cases, where UAA-A was the most frequently used tetranucleotide (49.7% in the slippery signal and 32.0% in the 'normal' termination signal) and UAG-G was the least frequently used (0.5% in the slippery signal and 1.8% in the 'normal' termination signal). However, the usage frequency of UAA-A (49.7%) was considerable higher than that of UAA-U (16.9%) in the slippery signals, even though they have similar frequencies in the "normal" termination signals (32.0% vs.

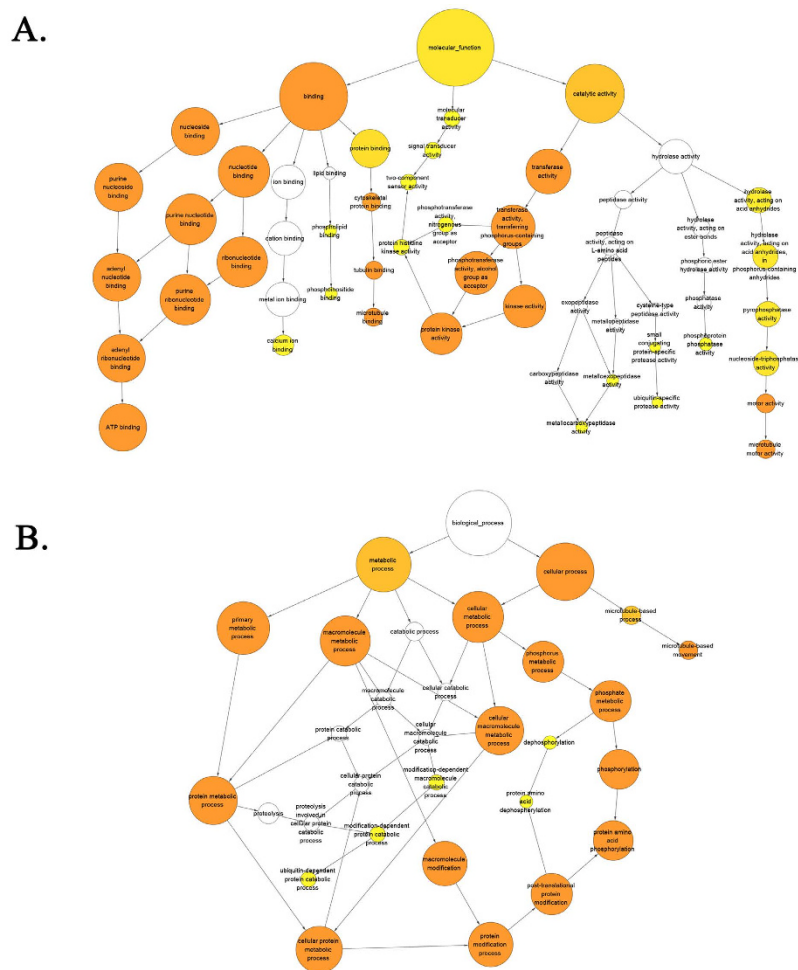


Figure 3. Enriched GO terms of +1 PRF transcripts were analyzed with Bingo. Each circle represents a GO term, arrows indicate pairs of GO terms with a parent-child relationship. Colored circles are statistically significant overrepresented GO terms (functions); the deeper of the color, the smaller the corrected p-value (more significant). Overrepresented molecular functions (A) and biological processes (B).

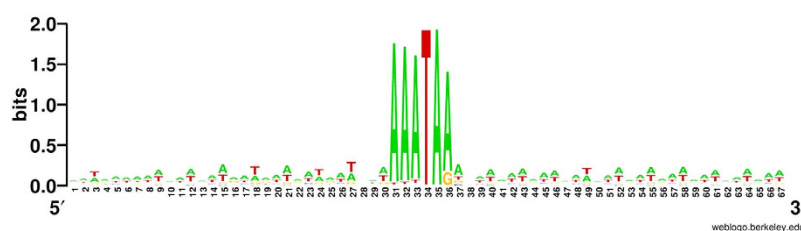


Figure 4. WebLogo displaying conserved sequences associated with frameshift sites. Sizes of letters denote information content, or sequence conservation, at each position. The analysis is based on the alignment of 30 bp preceding and following the frameshift motif from 4,545 predicted slippery sites.

31.0%). These results suggest that the tetranucleotide sequence UAA-A may be favourable for frameshifting in *E. octocarinatus*.

While no suppressor tRNA of UAA had been previously reported in *Euplotes*, a putative suppressor tRNA of UAA (Contig36094) was predicted from the genomic sequences of *E. octocarinatus*. Contig36094 (343 bp) was predicted to encode a 72 nucleotide tRNA that can fold into the characteristic cloverleaf secondary structure (Fig. 6B). An intervening sequence of 11 base pairs located at the canonical 37/38 position³⁹ was also predicted in this gene (Fig. 6A). The gene contains the characteristic internal split promoter and a typical termination signal⁴⁰ (Fig. 6A). Furthermore, a perfect consensus sequence, ‘TATAAAA’, for the TATA-binding protein (TBP) was located at position -35 to -29 relative to the +1 nt of the tRNA^{UAA}.

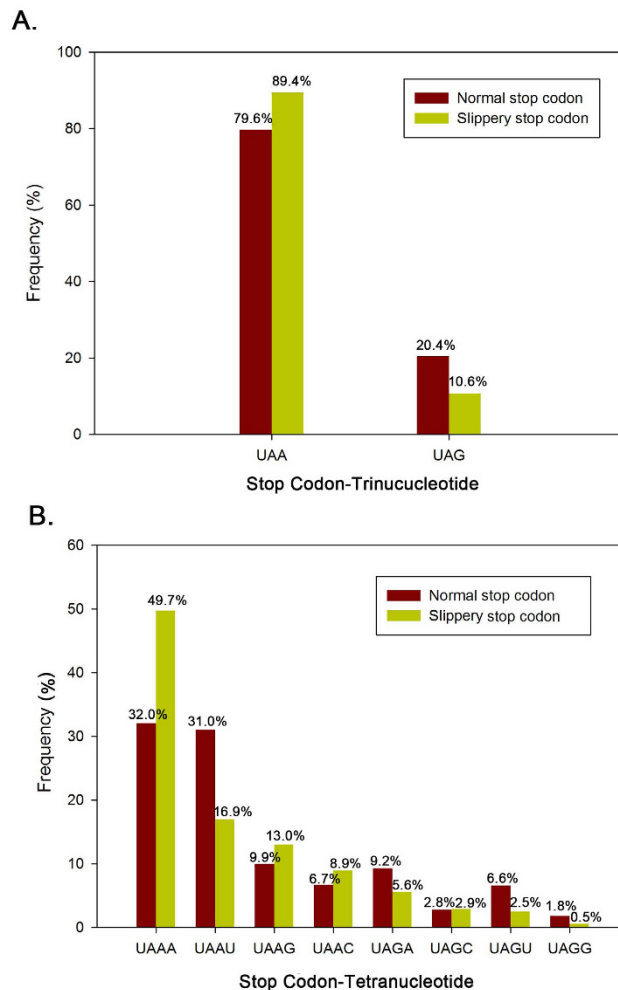


Figure 5. Frequency of stop codon usage in *Euplotes octocarinatus*. (A) Frequency of stop codon-trinucleotide. (B) Frequency of stop codon-tetranucleotide. The red and yellow bars indicate normal termination signal and slippery signal, respectively.

Further analysis indicated a base mismatch in the anticodon stem of the molecule, which increased the loop of unpaired bases from the typical seven to nine (Fig. 6B). Such an unusual structure was not unprecedented, and two examples of apparently nine-base anticodon loops in presumably wild-type, functional tRNAs were observed, namely, a tRNA^{Leu} in *Schizosaccharomyces pombe*⁴¹ (Fig. 6C) and a tRNA^{Met} in *Astasia longa*⁴² (Fig. 6D). In addition, the similar suppressor tRNAs that have been isolated from both bacteria^{43–46} and yeast^{47,48}, contained additional nucleotides in their anticodon loops. Expanded or modification-deficient anticodon stem loops have been proven to cause the ribosome to decode four rather than three nucleotides, resulting in a +1 translational frameshifting^{49–51}. Therefore, we proposed that the particular suppressor tRNA^{UAA} enters the ribosomal A site and decode 4 nucleotides when the translating ribosome meets the slippery stop codon. Then translation would continue in the +1 frame. Further experimental verification is needed to investigate how suppressor tRNA^{UAA} regulates +1 PRF in *E. octocarinatus*.

Conclusions

We reported a genome-wide investigation of +1 PRF in *E. octocarinatus* on the basis of its genome and transcriptome sequencing. We identified 3,700 (about 11%) putative +1 PRF genes, which to the best of our knowledge, is the highest frequency of +1 PRF found in all living organisms up to date. We also found a novel suppressor tRNA of UAA, which is potentially the key factor of +1 PRF in euplotids. This work provided the first comprehensive genome-wide investigation of +1 PRF and contributed to the mechanism of underlying programmed translational frameshift.

Methods

Cell culture, DNA isolation, and genome sequencing. *E. octocarinatus* line 69 was cultured in 2 liter flasks containing in synthetic medium⁵² at room temperature with the photosynthetic flagellate *Chlorogonium elongatum* as a food source. This strain was kindly provided by Klaus Heckmann (Universität Münster, Germany). Prior to harvesting, *Euplotes* cells were starved for 7–10 days to allow them to exhaust most of the food. Then,

A. Nucleotide sequence of Contig36094

```

>Contig36094
CCCCAAAACCCCAAAACCCCAAAACCCCAAAACCCCATGGAGAAATATGAAGGTTGAAAAGATTATAAGTAATAAATAAG
GTGCATAATAGCAATGTATAGATATCGTATAAAAGCATTGGTTTAAAGTTGTTAAGCAGCTGAAATAGITTAAGTGG
                                     TATA-box                                     A-box
TAGAACATCAGAATTTAAAGCATTTCAAACCCCTGAAGATGTAGGTTGACTCCCTACATTTCAGCGCTTTTATTCCGAGC
      Anti-codon                                     B-box                                     Termination signal
TTTATAACCATATCTTTATTCCATCATTCTATTTGCTAGTTTATTCAATTAATAATTTGGCTAAAGGGGTTTGGGG
TTTGGGGTTTGGGGTTTGGGG
  
```

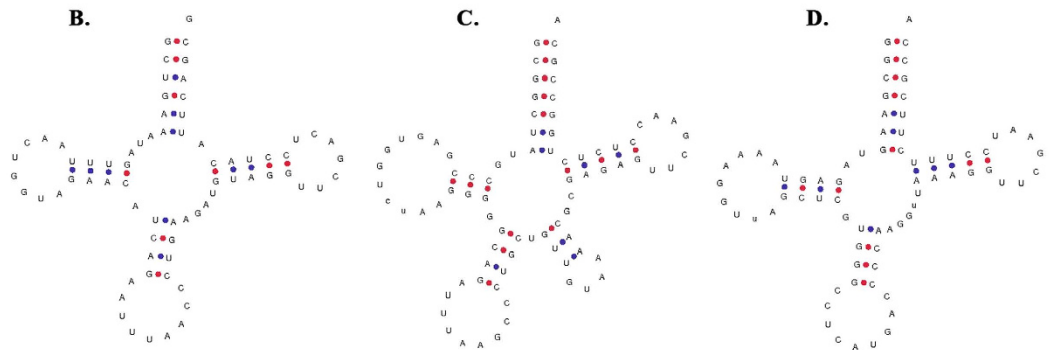


Figure 6. Nucleotide sequences of novel tRNA from different eukaryotic organisms shown in the cloverleaf arrangement. (A) The nucleotide sequence of Contig36094 is shown. The coding region is indicated by bold face and the terminal C_4A_4 and G_4T_4 telomeric sequences are shown in italic. The intragenic promoter boxes, the termination signal and a putative binding for the TATA-box binding protein are underlined. The putative intron is shown in red. The predicted cloverleaf structures of three novel tRNAs from (B) *Euplotes octocarinatus* (C) *Schizosaccharomyces pombe* and (D) *Astasia longa* are shown.

8–10 liters of starved cells were harvested by filtering through several layers of gauze to remove large particles, and then a filter paper was used to concentrate cells and remove bacteria and small contaminants. Cells were collected by centrifugation (4 °C, 4,000 rpm, 5 min) and then lysed in Urea buffer (0.01 M Tris-HCl, 0.01 M EDTA, 0.35 M NaCl, 1% SDS, 42% Urea, pH 7.4) for 5 min at 4 °C. After phenol/chloroform extraction, total DNA was dialyzed against isopropanol followed by ethanol precipitation. RNase was then added and incubated for 1 hr at 37 °C.

According to the whole genome shotgun strategy, genomic DNA was broken into random fragments. Two libraries with different paired-end (PE) length distributions were created from *Euplotes* DNA sequence data (Table S1). The 500 bp library was sequenced using the Illumina MiSeq platform, and the 180 bp library was sequenced using the Illumina HiSeq 2000 platform.

The genome assembly and assembly cleanup. The genome was assembled by a meta-assembly method (Fig. S1). All sequence data were used to build a reference genome.

MiSeq reads were assembled with Mira (4.0)⁵³. High quality reads were selected for assembly. Read1 and Read2 were trimmed by fastx_trimmer (from the FASTX-Toolkit) with the parameters -l 290 and -l 250, respectively, and then filtered by fastq_quality_filter (from the FASTX-Toolkit) with the parameters -q 20 -p 80. FLASH (1.2.10)⁵⁴ was used to merge these processed paired-end reads with the parameters -M 100. Finally, approximately 3.5 Gb reads were assembled with Mira (default parameters). SPAdes (2.5.0)⁵⁵ was run with the “careful” option on HiSeq reads. Then we merged two assembly results with the CAP3 assembler with strict overlap parameters (-o 50 -p 99).

To remove redundant contigs from the assembly, LASTZ⁵⁶ was used to align every contig to each other. Contigs were discarded (13,623 in total) if they had longer non-self matches that are identical or almost identical ($\geq 90\%$ coverage and $\geq 90\%$ sequence identical) (Fig. S1).

The final assembly contained a mixture of bacterial DNA and mitochondrial DNA. To identify bacterial genomic sequences, all telomereless contigs were searched against NCBI non-redundant protein sequences database using BLASTX (E-value $\leq 1e^{-5}$). Any contig that belongs to bacteria or archaea was removed. To exclude mitochondrial contamination in our final assembly, these telomereless contigs which had substantial TBLASTX matches (E-value $\leq 1e^{-4}$) to the *Euplotes minuta* and *Euplotes crassus* mitochondrial genome⁵⁷ were removed. A total of 1628 bacterial contigs and 72 mitochondrial contigs were identified and removed. In addition, we also removed 35 contigs that were shorter than 100 bp.

Assessment of genome completeness. To assess the completeness of the draft *Euplotes* macronuclear genome, we used a strategy similar to that used to assess completeness of *Oxytricha*³⁰.

Firstly, we evaluated the percentage of reads mapping to the final assembly. All reads and reads containing telomere sequences of HiSeq reads were separately mapped to the final assembly with BWA⁵⁸ (default parameters; version 0.7.5). Nearly all high-quality reads mapped to our final assembly (96% of all PE reads and 92% of

telomeric reads). Furthermore, the majority of contigs (70.1%) had both 5' and 3' telomeres (Table 1). This simple assessment indicated that our assembly was largely complete.

Then we analyzed the completeness of two gene sets: ribosomal proteins and tRNAs. Based on the reciprocal blast results, all 80 of the standard eukaryotic ribosomal proteins except L41 were identified (32 small subunit and 47 large subunit proteins). Considering that the coding sequence of human L41 is too short (only 75 bp), we speculated that the L41 of *Euplotes* probably was missed in the process of library construction. In addition, tRNAscan (version 1.3.1)⁵⁹ with default parameters was used to search for tRNAs. A total of 95 contigs of *Euplotes*'s macronuclear genome encode a comprehensive set of tRNAs for all 20 standard amino acids (Table S6) including a novel suppressor tRNAs of traditional stop codon UAA.

We also assessed the completeness of the macronuclear genome by searching protein sequences from *Euplotes* against the core eukaryotic genes (CEGs)⁶⁰. Matches from BLASTP with E-values lower than 1e-10 and a sequence coverage $\geq 70\%$ of the CEG sequence were counted as a match. Of the predicted proteins, 218 proteins were predicted for *Euplotes* and had substantial sequence similarity to the CEG protein sequences. 21 of the 30 remaining CEGs were found by TBLASTN matches or using HMMER3⁶¹ domain searches because of the deep evolutionary divergences of ciliates from these eukaryotes. After these more sensitive searches in *Euplotes*, only 6 CEGs are missing from the 245 ciliate-specific CEGs. Of the six undetectable ciliate-specific CEGs, one, KOG3285, is also missing from *Oxytricha*³⁰ and *Stylonychia*³¹. Thus, the macronuclear genomes of *Euplotes* encode 97.6% of the ciliate-specific CEGs.

RNA isolation and transcriptome sequencing. Cell culture and collection were the same as described for DNA isolation. Total RNA was extracted using the RNeasy Plus Mini Kit Cell Mini Kit (Qiagen) per manufacturer's instructions. Total RNA concentrations was determined using Qubit RNA Assay Kit in Qubit 2.0 Fluorometer (Life Technologies, CA, USA) and RNA integrity was assessed using the RNA Nano 6000 Assay Kit of the Agilent Bioanalyzer 2100 system (Agilent Technologies, CA, USA).

Poly-A mRNAs was purified using Dynal magnetic beads (Invitrogen). Double-stranded cDNAs were synthesized using reverse transcriptase and random hexamer primers. cDNAs were fragmented by nebulization, and the standard Illumina protocol was followed thereafter to construct mRNA-seq libraries. The normalized cDNA population was sequenced using the Illumina 2000 platform, with paired-end 125 bp mode. About 4.9 Gb of raw RNA-seq data were obtained.

Gene prediction. Given that the existence of PRF genes will influence the accuracy of gene prediction, all +1 PRF candidate genes were excluded. The *de novo* prediction software AUGUSTUS (version 3.0.2)⁶² was used to predict complete genes on the non-PRF contigs (38,615 in total).

To obtain a reliable training data set, all non-PRF transcripts of Cufflinks³³ assembly were aligned to the *Euplotes* macronuclear genome and reassembled by PASA (version r20140417, run with default parameters)⁶³. These transcripts which were marked as "complete" (had both ATG and TAA/TAG) were searched against NCBI non-redundant protein sequences database using BLASTX. Matches from BLASTX with E-values lower than 1e-10 and a sequence coverage $\geq 95\%$ of the top hit sequence were extracted. In addition, we only chose proteins that were < 70% identical to each other according to the recommendations in the AUGUSTUS documentation. Ultimately, 551 *Euplotes* genes were used to train AUGUSTUS. The final data set of 551 genes was split into training and test data sets of 401 and 150 genes respectively. For gene prediction, AUGUSTUS was run with the following parameters: "-species=euplotes -UTR=on -extrinsicCfgFile=install/augustus.3.0.2/config/extrinsic/extrinsic.M.R.M.E.W.cfg -genemodel=complete -codingseq=on". To produce additional constraints (hints) for AUGUSTUS, the RNA-seq data were processed according to the instructions on the website (<http://www.molecularevolution.org/molevolfiles/exercises/augustus/prediction.html#preprints>). We also recompiled AUGUSTUS after decreasing the default minimum length of intron hints in the source code from 39 to 25 bp to allow AUGUSTUS to evaluate hints for shorter introns³⁰.

Overall, 29,076 putative protein-coding genes were obtained, and 90% of them were supported by RNA-Seq Reads. About 89% nanochromosomes were predicted containing one or more complete gene. Key properties of *Euplotes*'s gene predictions are given in Table S7. Like other ciliates, the noncoding regions of *Euplotes* are more AT-rich than coding regions (e.g., 23.3% GC content in introns, versus 31.3% GC content in exons).

Functional annotation and enrichment analysis. The 'T' of the stop codon within the slippery sequence was artificially removed. Then these new *fs*-genes and non-PRF transcripts were translated into amino acid sequences using the GetOrf program in the EMBOSS package⁶⁴ with the *Euplotid* Nuclear Code, and the longest CDSs were obtained by using a custom Perl script. Subsequently, the amino acid sequences were loaded into Pfamscan⁶⁵ to perform protein domain annotation, and only Pfam-A database was searched.

Gene ontology (GO) annotations were performed by mapping of GO terms to Pfam entries. This mapping was generated from data supplied by InterPro⁶⁶ for the InterPro2GO mapping. Functional enrichment analysis of +1 PRF genes was performed to determine the significantly enriched GO terms and relevant proteins by using BINGO⁶⁷ plugin in the Cytoscape platform (version 3.1.1)⁶⁸. Enrichment analysis of GO term assignment was performed in reference to the entire *E. octocarinatus* transcripts (containing 7,060 proteins). The corrected (corr) p-values were derived from a hypergeometric test followed by Benjamini and Hochberg false discovery rate (FDR) correction. The FDR ≤ 0.05 was regarded as significant.

In addition, the +1 PRF transcripts were annotated according to the Kyoto Encyclopedia of Genes and Genomes (KEGG)³⁵ orthology (KO) using the KEGG Automatic Annotation Server (KAAS)⁶⁹. The amino acid sequences of translated +1 PRF transcripts were used as the query sequence, and the bi-directional best hit (BBH) method was employed to obtain the KO terms for the query sequences.

Availability of supporting data. The BioProject accession number for the genome is PRJNA294366. The raw genome sequences reads have been deposited in Sequence Read Archive (SRA) under accession SRX1267944 and SRX1270715. Transcriptome data has also been deposited in SRA under accession SRX1270740.

References

1. Tan, M., Brünen-Nieweler, C. & Heckmann, K. Isolation of micronuclei from *Euplotes octocarinatus* and identification of an internal eliminated sequence in the micronuclear gene encoding γ -tubulin 2. *European Journal of Protistology* **35**, 208–216 (1999).
2. Klobutcher, L. A. & Prescott, D. M. *The molecular biology of ciliated protozoa*. Academic Press, New York, 111–154 (1986).
3. Ghosh, S., Jaraczewski, J. W., Klobutcher, L. A. & Jahn, C. L. Characterization of transcription initiation, translation initiation, and poly(A) addition sites in the gene-sized macronuclear DNA molecules of *Euplotes*. *Nucleic Acids Research* **22**, 214–221 (1994).
4. Meyer, F. *et al.* UGA is translated as Cysteine in pheromone-3 of *Euplotes octocarinatus*. *Proc Natl Acad Sci. USA* **88**, 3758–3761 (1991).
5. Turanov, A. A. *et al.* Genetic code supports targeted insertion of two amino acids by one codon. *Science* **323**, 259–261 (2009).
6. Klobutcher, L. A. Sequencing of random *Euplotes crassus* macronuclear genes supports a high frequency of +1 translational frameshifting. *Eukaryotic Cell* **4**, 2098–2105 (2005).
7. Caliskan, N., Peske, F. & Rodnina, M. V. Changed in translation: mRNA recoding by –1 programmed ribosomal frameshifting. *Trends in Biochemical Sciences* **40**, 265–274 (2015).
8. Namy, O., Rousset, J.-P., Naphthine, S. & Brierley, I. Reprogrammed genetic decoding in cellular gene expression. *Mol Cell* **13**, 157–168 (2004).
9. Cobucci-Ponzano, B., Rossi, M. & Moracci, M. Translational recoding in archaea. *Extremophiles* **16**, 793–803 (2012).
10. Baranov, P. V., Gesteland, R. F. & Atkins, J. F. Recoding: translational bifurcations in gene expression. *Gene* **286**, 187–201 (2002).
11. Jacobs, J. L., Belew, A. T., Rakauskaitė, R. & Dinman, J. D. Identification of functional, endogenous programmed –1 ribosomal frameshift signals in the genome of *Saccharomyces cerevisiae*. *Nucleic Acids Research* **35**, 165–174 (2007).
12. Craigen, W. J. & Caskey, C. T. Expression of peptide chain release factor 2 requires high-efficiency frameshift. *Nature* **322**, 273–275 (1986).
13. Bekaert, M., Atkins, J. F. & Baranov, P. V. ARFA: a program for annotating bacterial release factor genes, including prediction of programmed ribosomal frameshifting. *Bioinformatics* **22**, 2463–2465 (2006).
14. Ivanov, I. P. & Atkins, J. F. Ribosomal frameshifting in decoding antizyme mRNAs from yeast and protists to humans: close to 300 cases reveal remarkable diversity despite underlying conservation. *Nucleic Acids Research* **35**, 1842–1858 (2007).
15. Kurian, L., Palanimurugan, R., Gödderz, D. & Dohmen, R. J. Polyamine sensing by nascent ornithine decarboxylase antizyme stimulates decoding of its mRNA. *Nature* **477**, 490–U147 (2011).
16. Adamski, F. M., Donly, B. C. & Tate, W. P. Competition between frameshifting, termination and suppression at the frameshift site in the *Escherichia coli* release factor-2 mRNA. *Nucleic Acids Research* **21**, 5074–5078 (1993).
17. Dinman, J. D. Mechanisms and implications of programmed translational frameshifting. *Wiley interdisciplinary reviews. RNA* **3**, 661–673 (2012).
18. Rom, E. & Kahana, C. Polyamines regulate the expression of ornithine decarboxylase antizyme *in vitro* by inducing ribosomal frameshifting. *Proc Natl Acad Sci. USA* **91**, 3959–3963 (1994).
19. Doak, T. G., Witherspoon, D. J., Jahn, C. L. & Herrick, G. Selection on the genes of *Euplotes crassus* Tec1 and Tec2 transposons: Evolutionary appearance of a programmed frameshift in a Tec2 gene encoding a tyrosine family site-specific recombinase. *Eukaryotic Cell* **2**, 95–102 (2003).
20. Jahn, C. L., Doktor, S. Z., Frels, J. S., Jaraczewski, J. W. & Krikau, M. F. Structures of the *Euplotes crassus* Tec1 and Tec2 elements - Identification of putative transposase coding regions. *Gene* **133**, 71–78 (1993).
21. Tan, M., Heckmann, K. & Brünen-Nieweler, C. Analysis of micronuclear, macronuclear and cDNA sequences encoding the regulatory subunit of cAMP-dependent protein kinase of *Euplotes octocarinatus*: Evidence for a ribosomal frameshift. *Journal of Eukaryotic Microbiology* **48**, 80–87 (2001).
22. Tan, M., Liang, A., Heckmann, K. & Brünen Nieweler, C. Programmed translational frameshifting is likely required for expressions of genes encoding putative nuclear protein kinases of the ciliate *Euplotes octocarinatus*. *Journal of Eukaryotic Microbiology* **48**, 575–582 (2001).
23. Aigner, S. *et al.* *Euplotes* telomerase contains an La motif protein produced by apparent translational frameshifting. *Embo J* **19**, 6230–6239 (2000).
24. Vallesi, A., Di Pretoro, B., Ballarini, P., Apone, F. & Luporini, P. A novel protein kinase from the ciliate *Euplotes raikovi* with close structural identity to the mammalian intestinal and male-germ cell kinases: Characterization and functional implications in the autocrine pheromone signaling loop. *Protist* **161**, 250–263 (2010).
25. Candelori, A., Luporini, P., Alimenti, C. & Vallesi, A. Characterization and expression of the gene encoding *En-MAPK1*, an intestinal cell kinase (ICK)-like kinase activated by the autocrine pheromone-signaling loop in the polar ciliate, *Euplotes nobilii*. *International Journal of Molecular Sciences* **14**, 7457–7467 (2013).
26. Karamysheva, Z. *et al.* Developmentally programmed gene elimination in *Euplotes crassus* facilitates a switch in the telomerase catalytic subunit. *Cell* **113**, 565–576 (2003).
27. Möllenbeck, M., Gavin, M. C. & Klobutcher, L. A. Evolution of programmed ribosomal frameshifting in the *TERT* genes of *Euplotes*. *Journal of Molecular Evolution* **58**, 701–711 (2004).
28. Wang, L., Dean, S. R. & Shippen, D. E. Oligomerization of the telomerase reverse transcriptase from *Euplotes crassus*. *Nucleic Acids Research* **30**, 4032–4039 (2002).
29. Martin, J. A. & Wang, Z. Next-generation transcriptome assembly. *Nature Reviews Genetics* **12**, 671–682 (2011).
30. Swart, E. C. *et al.* The *Oxytricha trifallax* macronuclear genome: a complex eukaryotic genome with 16,000 tiny chromosomes. *PLoS Biology* **11**, e1001473 (2013).
31. Aeschlimann, S. H. *et al.* The draft assembly of the radically organized *Stylonychia lemnae* macronuclear genome. *Genome Biology and Evolution* **6**, 1707–1723 (2014).
32. Trapnell, C., Pachter, L. & Salzberg, S. L. TopHat: discovering splice junctions with RNA-Seq. *Bioinformatics* **25**, 1105–1111 (2009).
33. Trapnell, C. *et al.* Transcript assembly and quantification by RNA-Seq reveals unannotated transcripts and isoform switching during cell differentiation. *Nature Biotechnology* **28**, 511–515 (2010).
34. Antonov, I., Baranov, P. & Borodovsky, M. GeneTack database: genes with frameshifts in prokaryotic genomes and eukaryotic mRNA sequences. *Nucleic Acids Research* **41**, D152–156 (2013).
35. Ogata, H. *et al.* KEGG: Kyoto Encyclopedia of Genes and Genomes. *Nucleic Acids Research* **27**, 29–34 (1999).
36. Gavin E. Crooks, Gary Hon, John-Marc Chandonia & Brenner, A. S. E. WebLogo: A sequence logo generator. *Genome Research* **14**, 1188–1190 (2004).
37. Klobutcher, L. A. & Farabaugh, P. J. Shifty ciliates: frequent programmed translational frameshifting in *Euplotids*. *Cell* **111**, 763–766 (2002).
38. Vallabhaneni, H., Fan-Minogue, H., Bedwell, D. M. & Farabaugh, P. J. Connection between stop codon reassignment and frequent use of shifty stop frameshifting. *RNA* **15**, 889–897 (2009).

39. Marck, C. & Grosjean, H. tRNomics: analysis of tRNA genes from 50 genomes of Eukarya, Archaea, and Bacteria reveals anticodon-sparring strategies and domain-specific features. *RNA* **8**, 1189–1232 (2002).
40. Pavesi, A., Conterio, F., Bolchi, A., Dieci, G. & Ottonello, S. Identification of new eukaryotic tRNA genes in genomic DNA databases by a multistep weight matrix analysis of transcriptional control regions. *Nucleic Acids Research* **22**, 1247–1256 (1994).
41. Sumner-Smith, M. *et al.* The sup8 tRNA^{Leu} gene of *Schizosaccharomyces pombe* has an unusual intervening sequence and reduced pairing in the anticodon stem. *Mol Gen Genet* **197**, 447–452 (1984).
42. Siemeister, G., Buchholz, C. & Hachtel, W. Genes for the plastid elongation factor Tu and ribosomal protein S7 and six tRNA genes on the 73 kb DNA from *Astasia longa* that resembles the chloroplast DNA of *Euglena*. *Mol Gen Genet* **220**, 425–432 (1990).
43. Riddle, D. L. & Carbon, J. Frameshift suppression: a nucleotide addition in the anticodon of a glycine transfer RNA. *Nature: New Biology* **242**, 230–234 (1973).
44. Magliery, T. J., Anderson, J. C. & Schultz, P. G. Expanding the genetic code: selection of efficient suppressors of four-base codons and identification of “shifty” four-base codons with a library approach in *Escherichia coli*. *J Mol Biol* **307**, 755–769 (2001).
45. Sroga, G. E., Nemoto, F., Kuchino, Y. & Bjork, G. R. Insertion (sufB) in the anticodon loop or base substitution (sufC) in the anticodon stem of tRNA(Pro)₂ from *Salmonella typhimurium* induces suppression of frameshift mutations. *Nucleic Acids Research* **20**, 3463–3469 (1992).
46. Yourno, J. Externally suppressible +1 “glycine” frameshift: possible quadruplet isomers for glycine and proline. *Nature: New Biology* **239**, 219–221 (1972).
47. Cummins, C. M., Donahue, T. F. & Culbertson, M. R. Nucleotide sequence of the SUF2 frameshift suppressor gene of *Saccharomyces cerevisiae*. *Proc Natl Acad Sci. USA* **79**, 3565–3569 (1982).
48. Gaber, R. F. & Culbertson, M. R. Codon recognition during frameshift suppression in *Saccharomyces cerevisiae*. *Molecular and Cellular Biology* **4**, 2052–2061 (1984).
49. Maehigashi, T., Dunkle, J. A., Miles, S. J. & Dunham, C. M. Structural insights into +1 frameshifting promoted by expanded or modification-deficient anticodon stem loops. *Proc Natl Acad Sci. USA* **111**, 12740–12745 (2014).
50. Tuohy, T. M., Thompson, S., Gesteland, R. F. & Atkins, J. F. Seven, eight and nine-membered anticodon loop mutants of tRNA (2Arg) which cause +1 frameshifting. Tolerance of DHU arm and other secondary mutations. *J Mol Biol* **228**, 1042–1054 (1992).
51. Fagan, C. E., Maehigashi, T., Dunkle, J. A., Miles, S. J. & Dunham, C. M. Structural insights into translational recoding by frameshift suppressor tRNA^{Suf}. *RNA* **20**, 1944–1954 (2014).
52. Freiburg, M. Identification of cell surface polypeptides of the hypotrich ciliate *Euplotes octocarinatus*. *Arch. Protistenkd* **143**, 311–318 (1992).
53. Chevreur, B., Wetter, T. & Suhai, S. Genome sequence assembly using trace signals and additional sequence information. *German Conference on Bioinformatics*, 45–56 (1999).
54. Magoč, T. & Salzberg, S. L. FLASH: fast length adjustment of short reads to improve genome assemblies. *Bioinformatics* **27**, 2957–2963 (2011).
55. Bankevich, A. *et al.* SPAdes: a new genome assembly algorithm and its applications to single-cell sequencing. *Journal of Computational Biology* **19**, 455–477 (2012).
56. Harris, R. S. *Improved pairwise alignment of genomic DNA* Doctor of Philosophy thesis, Pennsylvania State University (2007).
57. De Graaf, R. M. *et al.* The mitochondrial genomes of the ciliates *Euplotes minuta* and *Euplotes crassus*. *BMC Genomics* **10**, 514 (2009).
58. Li, H. & Durbin, R. Fast and accurate short read alignment with Burrows-Wheeler transform. *Bioinformatics* **25**, 1754–1760 (2009).
59. Lowe, T. M. & Eddy, S. R. tRNAscan-SE: a program for improved detection of transfer RNA genes in genomic sequence. *Nucleic Acids Research* **25**, 955–964 (1997).
60. Tatusov, R. L. *et al.* The COG database: an updated version includes eukaryotes. *BMC Bioinformatics* **4**, 41 (2003).
61. Eddy, S. R. A new generation of homology search tools based on probabilistic inference. *Genome informatics. International Conference on Genome Informatics* **23**, 205–211 (2009).
62. Stanke, M. *et al.* AUGUSTUS: ab initio prediction of alternative transcripts. *Nucleic Acids Research* **34**, W435–439 (2006).
63. Haas, B. J. *et al.* Improving the *Arabidopsis* genome annotation using maximal transcript alignment assemblies. *Nucleic Acids Research* **31**, 5654–5666 (2003).
64. Rice, P., Longden, I. & Bleasby, A. EMBOSS: the European molecular biology open software suite. *Trends in Genetics* **16**, 276–277 (2000).
65. Finn, R. D. *et al.* The Pfam protein families database. *Nucleic Acids Research* **36**, D281–D288 (2008).
66. Mitchell, A. *et al.* The InterPro protein families database: the classification resource after 15 years. *Nucleic Acids Research* **43**, D213–221 (2015).
67. Maere, S., Heymans, K. & Kuiper, M. BiNGO: a Cytoscape plugin to assess overrepresentation of gene ontology categories in biological networks. *Bioinformatics* **21**, 3448–3449 (2005).
68. Shannon, P. *et al.* Cytoscape: a software environment for integrated models of biomolecular interaction networks. *Genome Research* **13**, 2498–2504 (2003).
69. Wu, J., Mao, X., Cai, T., Luo, J. & Wei, L. KOBAS server: a web-based platform for automated annotation and pathway identification. *Nucleic Acids Research* **34**, W720–724 (2006).
70. Saulquin, X. *et al.* +1 Frameshifting as a novel mechanism to generate a cryptic cytotoxic T lymphocyte epitope derived from human interleukin 10. *The Journal of Experimental Medicine* **195**, 353–358 (2002).
71. Ivanov, I. P., Gesteland, R. F. & Atkins, J. F. A second mammalian antizyme: Conservation of programmed ribosomal frameshifting. *Genomics* **52**, 119–129 (1998).
72. Ivanov, I. P., Rohrwasser, A., Terreros, D. A., Gesteland, R. F. & Atkins, J. F. Discovery of a spermatogenesis stage-specific ornithine decarboxylase antizyme: antizyme 3. *Proc Natl Acad Sci. USA* **97**, 4808–4813 (2000).
73. Matsufuji, S. *et al.* Autoregulatory frameshifting in decoding mammalian ornithine decarboxylase antizyme. *Cell* **80**, 51–60 (1995).
74. Nilsson, J., Koskineniemi, S., Persson, K., Grahn, B. & Holm, I. Polyamines regulate both transcription and translation of the gene encoding ornithine decarboxylase antizyme in mouse. *European Journal of Biochemistry* **250**, 223–231 (1997).
75. Ivanov, I. P., Matsufuji, S., Murakami, Y., Gesteland, R. F. & Atkins, J. F. Conservation of polyamine regulation by translational frameshifting from yeast to mammals. *Embo J* **19**, 1907–1917 (2000).
76. Saito, T. *et al.* Two zebrafish (*Danio rerio*) antizymes with different expression and activities. *Biochem J* **345**, 99–106 (2000).
77. Ivanov, I. P., Simin, K., Letsou, A., Atkins, J. F. & Gesteland, R. F. The *Drosophila* gene for antizyme requires ribosomal frameshifting for expression and contains an intronic gene for snRNP Sm D3 on the opposite strand. *Molecular and Cellular Biology* **18**, 1553–1561 (1998).
78. Morris, D. K. & Lundblad, V. Programmed translational frameshifting in a gene required for yeast telomere replication. *Curr Biol* **7**, 969–976 (1997).
79. Asakura, T. *et al.* Isolation and characterization of a novel actin filament-binding protein from *Saccharomyces cerevisiae*. *Oncogene* **16**, 121–130 (1998).
80. Zimmer, M., Sattelberger, E., Inman, R. B., Calendar, R. & Loessner, M. J. Genome and proteome of *Listeria monocytogenes* phage PSA: an unusual case for programmed +1 translational frameshifting in structural protein synthesis. *Molecular Microbiology* **50**, 303–317 (2003).
81. Firth, A. *et al.* Ribosomal frameshifting used in *influenza A virus* expression occurs within the sequence UCC_UUU_CGU and is in the +1 direction. *Open Biology* **2**, 120109 (2012).

Acknowledgements

This project is supported by grants from National Natural Science Foundation of China (No. 31372199) to A. Liang.

Author Contributions

A.L. and R.W. conceived and conducted the project. J.X. and W.M. guided data analysis. J.X. and W.W. participated in correcting the manuscript critically. R.W. wrote the manuscript. All authors have read and approved the final manuscript.

Additional Information

Supplementary information accompanies this paper at <http://www.nature.com/srep>

Competing financial interests: The authors declare no competing financial interests.

How to cite this article: Wang, R. *et al.* High frequency of +1 programmed ribosomal frameshifting in *Euplotes octocarinatus*. *Sci. Rep.* **6**, 21139; doi: 10.1038/srep21139 (2016).



This work is licensed under a Creative Commons Attribution 4.0 International License. The images or other third party material in this article are included in the article's Creative Commons license, unless indicated otherwise in the credit line; if the material is not included under the Creative Commons license, users will need to obtain permission from the license holder to reproduce the material. To view a copy of this license, visit <http://creativecommons.org/licenses/by/4.0/>